

Estimating the integral length scale on turbulent flows from the zero crossings of the longitudinal velocity fluctuation

D.O. Mora · M. Obligado

Received: date / Accepted: date

Abstract The integral length scale (\mathcal{L}) is considered to be characteristic of the largest motions of a turbulent flow, and as such, it is an input parameter in modern and classical approaches of turbulence theory and numerical simulations. Its experimental estimation, however, could be difficult in certain conditions, for instance, when the experimental calibration required to measure \mathcal{L} is hard to achieve (hot-wire anemometry on large scale wind-tunnels, and field measurements), or in ‘standard’ facilities using active grids due to the behaviour of their velocity autocorrelation function $\rho(r)$, which does not in general cross zero. In this work, we provide two alternative methods to estimate \mathcal{L} using the variance of the distance between successive zero crossings of the streamwise velocity fluctuations, thereby reducing the uncertainty of estimating \mathcal{L} under similar experimental conditions. These methods are applicable to variety of situations such as active grids flows, field measurements, and large scale wind tunnels.

Keywords HIT, integral length scale, active grids

1 Introduction

The integral length scale (\mathcal{L}) is widely interpreted as the characteristic length scale of the energy containing eddies in a turbulent flow. \mathcal{L} is defined as the integral of the normalised velocity autocorrelation function; $\mathcal{L} = \int_0^\infty \rho(r) dr$, where $\rho(r) = \langle u'(x)u'(x+r) \rangle / \sigma_u^2$ [25], and σ_u is the standard deviation of the streamwise velocity fluctuations u' . Moreover, \mathcal{L} is central to different attempts aiming to understand turbulence evolution and its cascading process [20, 28]. For instance, for turbulence close to a statistically homogeneous and isotropic state (HIT), the dissipation constant $C_\epsilon = \epsilon \mathcal{L} / \sigma_u^3$, depends on two large scale quantities, \mathcal{L} and σ_u .

D.O. Mora.

Université Grenoble Alpes, CNRS, Grenoble-INP, LEGI, F-38000, Grenoble, France and University of Washington, Department of Mechanical Engineering, Seattle, USA

M. Obligado

Université Grenoble Alpes, CNRS, Grenoble-INP, LEGI, F-38000, Grenoble, France E-mail: Martin.Obligado@univ-grenoble-alpes.fr

In experiments, noise and non-stationary experimental conditions can pollute the large separation values, which are denoted by increments of r . This prevents the computation of the integral $\int_0^\infty \rho(r)dr$ up to infinity. Therefore, the value of \mathcal{L} is usually estimated by different methods. These include: integrating up to the first zero crossing [18]; integrating up to a minimum value of the autocorrelation function [18, 26]; integrating up to the value where the autocorrelation falls below e^{-1} [18, 2] or via standard Kolmogorov scalings. Valente & Vassilicos [27] also propose to integrate the autocorrelation function up to a lengthscale which is about ten times \mathcal{L} . Moreover, Krogstad & Davidson [11] suggest to apply a high-pass filter to the time signal at 0.1 Hz to counteract the effect of non-stationary low frequencies on the estimation of \mathcal{L} . These previous estimations are usually accompanied by the assumption that Taylor's hypothesis holds, $r = U\tau$, where τ refers to time and U is the local convective velocity.

Despite their widespread use, these approaches to estimate \mathcal{L} may fail or result in ambiguities. For instance, some experimental studies using facilities that generate turbulence by means of active grids [17] have reported that $\rho(r)$ sometimes does not decay exponentially nor cross zero [21, 16]. These observations pose the problem of how to compute \mathcal{L} under such conditions. Likewise, in large scale experiments [8], or in field measurements, conducting the equipment calibration procedure could be very cumbersome, and therefore, such uncertainty would contaminate the reported values of the turbulent quantities.

To cater for the autocorrelation behaviour, Puga & LaRue [21] have recommended estimating the integral length scale as $\mathcal{L} = \int_0^{r_0} \rho(r)dr$ with $r_0 = U\tau_0 = U\tau(\rho(\tau) = \delta)$. The parameter δ quantifies the dispersion on the estimation of $\rho(r)$. It is usually found by averaging different segments extracted from the velocity time signal. Therefore, when $\int_0^{r_0} \rho(r)dr$ is estimated by this method, δ plays an important role in the value of \mathcal{L} obtained. Nevertheless, the choice of δ is ambiguous as it strongly depends on the averaging chosen for the computation of $\rho(r)$. This is not a minor issue considering the influence \mathcal{L} exerts on the normalised dissipation rate constant C_ε , e.g., Mora et al. [16] reported $C_\varepsilon \approx 0.3$ in disagreement (by a factor of 2) with the value $C_\varepsilon \approx 0.6$ reported by Puga & LaRue [21] for similar values of Re_λ , despite the high degree of turbulence isotropy and turbulence homogeneity present in both experiments.

Puga & LaRue [21] anticipated that their method could not be general to all active grid generated flows, as it has been reported that the active grid protocol could affect the largest scales of the flow [10, 9]. Then, the choice of δ , which under this method may change between different experimental conditions or data analyses, could impact \mathcal{L} and C_ε making it difficult to compare different results available in the literature.

To address this problem, we study the zero crossings of u' for different datasets. Zero crossing analysis has been used in the past to characterise the small scales features of the flow via the Taylor microscale (λ) [23, 12, 16]. Given that the zero crossings of a velocity signal usually do not depend on the equipment calibration (as far as the mean velocity is known), this analysis is suitable even under challenging experimental conditions.

The first approach proposed is solely based on the work of McFadden [13], whereas the second one relies on the observation that the velocity field filtered at a scale equal to the integral length scale seems to exhibit uncorrelated zero crossings. Both approaches are able to recover values of \mathcal{L} in several turbulent

flows in good agreement with previous established methods [18]. Finally, we also analyse the structure of the zero crossings for different turbulent signals by means of Voronoï tessellations [7, 14].

2 Methodology

We analysed measurements taken via hot-wire anemometry (HWA). These measurements, except for those using a passive grid (see table 1), have been previously published in the literature [5, 16], and span a variety of turbulent flows generated by different mechanisms (see table 1): downstream of active grids or passive grids, and downstream of the wake of an irregular bluff plate (figure 1a).

All grid experiments were conducted in the *Lespinard* wind tunnel in LEGI, a low-turbulence wind tunnel facility with a measurement cross section of 75×75 cm², which has been extensively used to conduct experiments under homogeneous isotropic turbulence conditions [16]. Measurements were taken 3 m downstream of the grid. The measuring instrument used to record the velocity fluctuations, was a single Dantec Dynamics 55P01 hot-wire probe, driven by a Dantec StreamLine constant temperature anemometer (CTA) system. The Pt-W wires were $5 \mu\text{m}$ in diameter, 3 mm long, with a sensing length of 1.25 mm. Acquisitions were made for 300s at 25kHz and 50 kHz. For all measurements reported here, the Kolmogorov frequency was always smaller than half our sampling frequency.

The wake experiments were conducted in the 3×3 wind tunnel at Imperial College London, using the same HWA system as in the grid experiments. Measurements were taken at the centreline at the streamwise distances $D = 15$ and $D = 50$ from a plate with a characteristic length $D = \sqrt{\mathcal{A}} = 64\text{mm}$ (with \mathcal{A} being the frontal area of the plate).

2.1 Zero crossings computation

For this study, we employed a Reynolds decomposition for the streamwise velocity ($u = U + u'(\tau)$), to extract the eulerian fluctuating velocity u' . We then computed the fluctuating velocity $u'(\tau)$ zero crossings, i.e., the set of times τ_i^c for which $u'(\tau_i^c) = 0$ (see top of figure 1b), and translated this list of zero crossings from time into space by assuming the Taylor hypothesis $Z_i = \tau_i^c U$ (see figure 1b). It was verified that all measurements had enough temporal resolution to estimate λ [16] via the zero crossings. A common procedure to verify the latter [23, 12] is as follows:

1. Take the acquired fluctuating velocity signal, and low pass filter it (with a high order filter, e.g. a fifth order butterworth filter) at different sizes $\eta_C = 2\pi/\kappa$ (where κ is the wave number), given the use of the Taylor hypothesis this is equivalent to filter at different *frequencies*.
2. Compute the signal zero crossings, and their number density (n_s = number of zeros/duration of the signal) at at each filter size (*frequency*).
3. If a plateau of n_s is present for filter scales smaller (*larger*) than a certain scale (*frequency*) η_C^* (not to be confused with the Kolmogorov length scale η), the value of n_s is properly resolved. One could then estimate λ via $n_s^{-1}|_* = \pi C \lambda$,

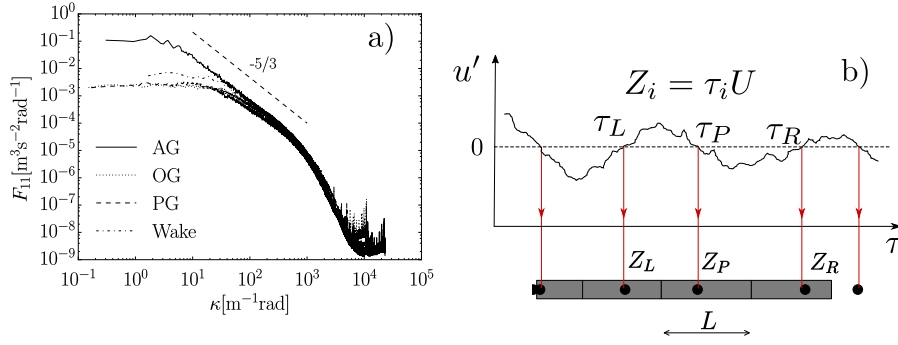


Fig. 1: a) Longitudinal energy density spectra (F_{11}) for the data found in table 1. b) Zero crossings and 1D Voronoi tessellation illustration. For a given zero crossing position Z_P with left, and right neighbour crossings Z_L , and Z_R respectively, the length of the Voronoi cell (centered on Z_P) is given by $L = |Z_R - Z_L|/2$.

Parameter	OG	AG	PG	Wake
U_∞ (m/s)	4.4–17.0	1.8–6.8	1.5–18.0	10.0
σ_u/U (%)	2.0–10.0	12.5–15.0	3.0–2.50	3.0–8.0
λ (mm)	8.0–3.0	16.0–9.0	9.0–4.0	10–5.4
Re_λ	50–200	200–731	30–130	200–300
η (μm)	400–100	500–180	918–191	340–163
\mathcal{L} (cm)	1.0–3.0	5.0–11.0	1.7–2.8	4–6.2

Table 1: Typical turbulence parameters range for the open (OG), active (AG) [16], and passive (PG) grids. AG refers to the active grid being operated in a random mode while *OG* to the same grid, completely open and static. We also employed records from the wake of an object [5]. In the table: inlet velocity U_∞ , turbulence intensity σ_u/U (with U the mean local velocity), Taylor micro-scale λ , Reynolds number based on the Taylor micro-scale $Re_\lambda = \lambda \sigma_u / \nu$ (ν being the kinematic viscosity of the flow), Kolmogorov length scale $\eta = (\nu^3/\varepsilon)^{1/4}$ and the streamwise integral length scale \mathcal{L} (obtained via $\rho(r)$).

with C being a constant in the order of unity which accounts for the non-gaussianity of the signal [12].

2.2 Variance of zero crossing successive intervals and \mathcal{L}

The seminal work of McFadden [13] was the first to derive for gaussian processes closed expressions to compute the variance of the interval distance between two successive zero crossings ($\Delta Z = Z_{i+1} - Z_i$) under two analytically tractable conditions: intervals between zeros are statistically independent, or intervals between zeros make a Markov chain. For the former, statistically independent case, the expression for the variance goes as,

$$\text{Var}(\Delta Z) = 2\langle \Delta Z \rangle \int_0^\infty \frac{2}{\pi} \arcsin(\rho(\tau)) d\tau. \quad (1)$$

The latter expression, and assuming Taylor hypothesis, provides an estimate for \mathcal{L} if the assumption of independent zero crossing intervals approximately holds for turbulent signals;

$$\frac{\text{Var}(\Delta Z)}{2\langle \Delta Z \rangle} = \int_0^\infty \frac{2}{\pi} \arcsin(\rho(\tau)) d\tau = \int_0^\infty \frac{2}{\pi} \left(\rho(\tau) + \frac{\rho(\tau)^3}{6} + \frac{\rho(\tau)^5}{40} + \dots \right) \leq \int_0^\infty \rho(\tau) d\tau. \quad (2)$$

By truncating the integral up to the first term, one obtains a relation between the Fano factor [22], and the integral time (\mathcal{T}) and length scales:

$$\frac{\pi}{4} \frac{\text{Var}(\Delta Z)}{\langle \Delta Z \rangle} \approx \int_0^\infty \rho(\tau) d\tau = \mathcal{T} = \mathcal{L}/U. \quad (3)$$

2.3 Successive zero crossings and 1D Voronoï tessellation

Interestingly, if McFadden's assumption of statistically independent intervals holds, the variance of the length between two successive intervals [1] could be written as,

$$\text{Var}(\Delta Z_1 + \Delta Z_2) = \text{Var}(\Delta Z_1) + \text{Var}(\Delta Z_2) + \text{Cov}(\Delta Z_1, \Delta Z_2). \quad (4)$$

Thus, an easy way to analyse the implications of this assumption (and its deviations) could be using 1D Voronoï tessellations [7]. These two frameworks (Voronoi tessellations and 'raw' inter-crossing distances) are related by their respective definitions. For instance, if a random variable ΔZ represents the distance between successive crossings, the respective Voronoï cell length L (also a random variable) is given by $L = 1/2(\Delta Z_L + \Delta Z_R)$, where $\Delta Z_L = |Z_P - Z_L|$ and $\Delta Z_R = |Z_R - Z_P|$ are the crossing lengths (random variables) at the left, and at the right of the crossing Z_P (see figure 1b). From these definitions; $\langle L \rangle = \langle \Delta Z \rangle = n_s^{-1}$.

Then, if the covariance between ΔZ_L and ΔZ_R is very weak, the variance of the ensemble of normalized Voronoï cells ($\mathcal{V} = L/\langle L \rangle$) is half the variance of $\Delta Z/\langle \Delta Z \rangle^2$:

$$\frac{1}{2} \frac{\text{Var}(\Delta Z)}{\langle \Delta Z \rangle^2} = \frac{\text{Var}(L)}{\langle L \rangle^2} = \sigma_{\mathcal{V}}^2. \quad (5)$$

The latter expression is easily verified for a random Poisson process (RPP), for which $\langle \Delta Z \rangle = 1$, $\text{Var}(\Delta Z) = 1$, and its respective Voronoï normalised cell variance is $\text{Var}(L)/\langle L \rangle^2 = 1/2$ [7]. We will refer to the standard deviation of this RPP process as $\sigma_{RPP} = \sqrt{1/2}$, and to the respective standard deviation coming from our Voronoï analysis of turbulent signals as $\sigma_{\mathcal{V}}$.

3 Results

3.1 Estimation of \mathcal{L} via the McFadden equation

We compute the values of $\text{Var}(\Delta Z)$ and $\langle \Delta Z \rangle$ for all datasets and examine the accuracy of McFadden's equation (equation 3). To estimate $\text{Var}(\Delta Z)$ and $\langle \Delta Z \rangle$, we follow a standard procedure found in the literature [23, 12], and described in section 2.1: we low-pass filter u' with a range of filter sizes η_C , and compute the signal zero crossings and zero crossings density at each filter size. The presence of a plateau (not reported here, but present for all our datasets) for small values of η_C show that n_s is well resolved, and therefore λ can be computed as $n_s^{-1} = \langle \Delta Z \rangle \sim \pi\lambda$. Resolving λ gives credence to the use of McFadden's equation with our datasets values.

To check the validity of McFadden's equation, we apply it to all velocity signals and for all filter scales (see figure 2). The equation provides indeed an acceptable estimation of \mathcal{L} for large values of Re_λ when the value at the plateau is compared to the traditional method of integrating up to the first zero of the autocorrelation.

Our method, however, has a residual dependency on Re_λ coming from variance value at the plateau, and as expected from previous analyses [12]. On the other hand, for the AG data (figure 2d), our results suggest that there was indeed a underestimation of the original values of $\mathcal{L} = \int_0^{r_0} \rho(r) dr$ (already discussed in [16]), and such underestimation strongly depends on the value of δ selected; as δ increases \mathcal{L} decreases.

Moreover, these observations advance that indeed the assumption of independent successive zero crossings could hold to some extent in turbulent signals. In fact, if equation 4 is approximately valid at all filters of interest, then the same follows for equation 5, which relates the variance of the Voronoï tessellation σ_V^2 applied to zero crossings with the variance of the interval distance between two successive zero crossings $\text{Var}(\Delta Z)$. The latter yields $\text{Var}(L) = \frac{1}{2}\text{Var}(\Delta Z)$. Equation 5 then (see figures 3a to 3d) gives:

$$0.90 < \sigma_V^2 / \left(\frac{1}{2} \frac{\text{Var}(\Delta Z)}{\langle \Delta Z \rangle^2} \right) = \left(\frac{\text{Var}(L)}{\langle L \rangle^2} \right) / \left(\frac{1}{2} \frac{\text{Var}(\Delta Z)}{\langle \Delta Z \rangle^2} \right) < 1.02, \quad (6)$$

at all filter scales of interest for the data found in Table 1. This observation supports that the independent interval assumption is approximately valid within 10% error for our datasets.

3.2 Voronoï analysis

Taking into account the previous section observations, we applied 1D Voronoï tessellation analysis [7] to the signals' zero crossings (see figure 1b) at each filter scale.

Our results reveal that σ_V (see figures 4a to 4d) has complex behaviour with the filter scale η_C which can be divided in 3 parts. First, a plateau regime at low values of $\kappa_C \sim \eta_C^{-1}$ representative of a flat white noise gaussian spectrum. Second, an intermediate regime where σ_V may attain a power law behaviour with an exponent close to 1/4 for large values of Re_λ ; despite of its persistence among different datasets, the existence of this intermediate regime remains unexplained

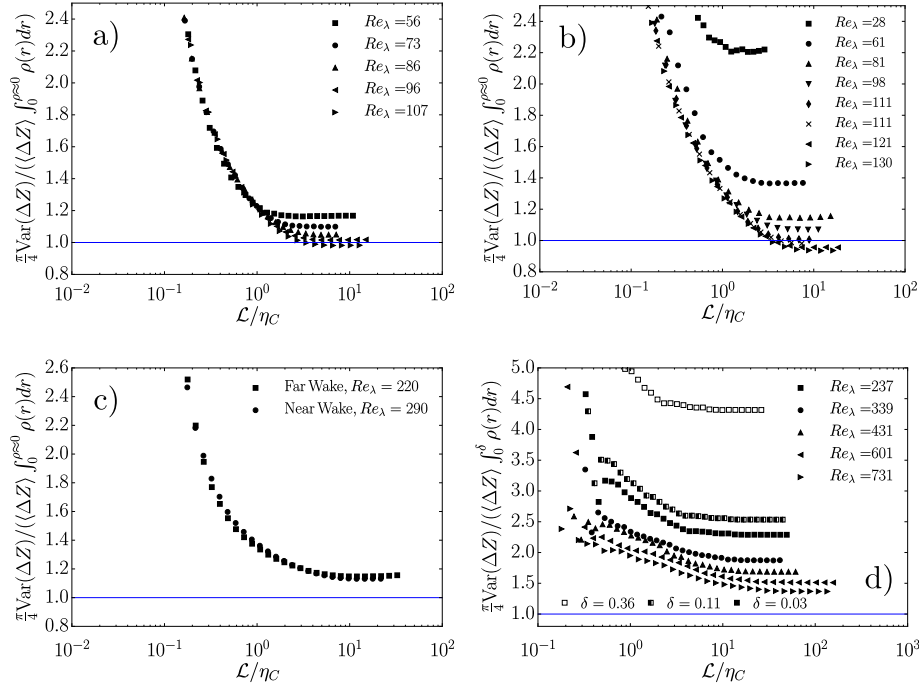


Fig. 2: Estimation of \mathcal{L} via equation 3. a) OG. b) PG. c) Wakes. d) AG. For the AG datasets [16], the autocorrelation integrals were estimated by the method of Puga and La Rue [21]. We also show the sensitivity of this parameter to different values of δ for the lowest value of Re_λ (\square).

and is left for future research as the limited extend of our data does not allows us to unambiguously conclude the accuracy of the exponent. Third, a second plateau consistent with the one found for the zero crossing number density $n_s^{-1} = \langle \Delta Z \rangle$ is found.

On the contrary, and interestingly, there seems to be a strong correlation between the filter scale at which $\sigma_V/\sigma_{RPP} \approx 1$, and \mathcal{L} , i.e., apparently $\sigma_V/\sigma_{RPP} \approx 1$ when $\eta_C = \mathcal{L}$. These results hint that an alternative definition of \mathcal{L} could be: the length-scale at which the zero crossing intervals topology is approximately uncorrelated.

Furthermore, a comparison between the values estimated from McFadden's equation (taking the last points of the plateaus of n_s , and σ_V), and the values extracted from $\sigma_V/\sigma_{RPP} \approx 1$ when $\eta_C = \mathcal{L}$ (see figures 2d and 5a) points out again that for the AG data, the integral length scale \mathcal{L} could have been originally underestimated by a factor of 2 explaining the discrepancy in C_ε between the studies of [16], and [21]. This underestimation occurs, when integrating the autocorrelation by the method proposed by [21], as a consequence of the arbitrary choice of the value δ ; smaller values converge to a closer value of \mathcal{L} , while larger values of δ reduce the noise while keeping the trends.

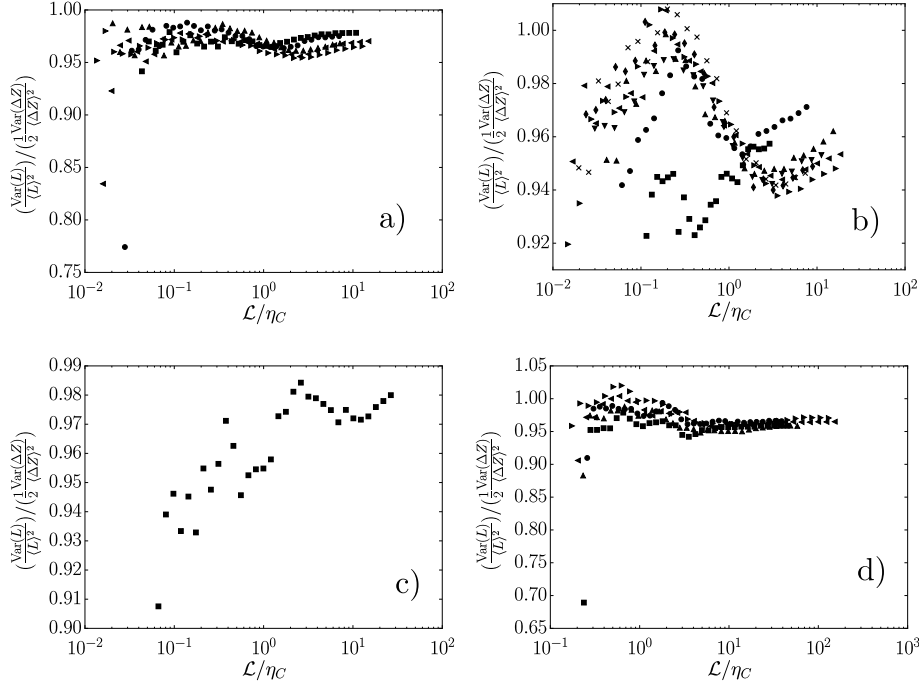


Fig. 3: Ratio between the variance of Voronoï cells $\text{Var}(L) = \langle (L - \langle L \rangle)^2 \rangle$, and the respective one of the interval distance between two successive zero crossings; $\text{Var}(\Delta Z) = \langle \Delta Z^2 \rangle - \langle \Delta Z \rangle^2$. Note that $\langle L \rangle = \langle \Delta Z \rangle$. a) OG. b) PG. c) Wakes. d) AG.

These observations suggest that the integral length scale can also be estimated as $\mathcal{L} = \mathcal{L}_{Voro} = \eta_C |_{\sigma_V \approx \sigma_{RPP}}$. This new definition (see figure 5b) seems to be less sensitive to Re_λ than the value of \mathcal{L} estimated from equation 3, and to have less dispersion. The values obtained by the latter method show that for grid turbulence at large U_∞ , \mathcal{L} increases with Re_λ , as previously reported.

On the other hand, and in the context of inertial particles clustering, Monchaux et al. [14] introduced Voronoï tessellations, and argued that clustering is present when the ratio $\sigma_V|_*/\sigma_{RPP} > 1$ (where $\sigma_V|_*$ is the value of σ_V at the plateau observed at small values of η_C), and its intensity depends on this ratio magnitude. Being the standard deviation mainly set by the ‘voids’ [24] (periods without zero crossings), our results show that the degree of clustering of zero crossings increases with $Re_\lambda^{1/3}$ (see figure 5c), in agreement with the observations of Mazellier and Vassilicos [12].

We therefore conclude that while McFadden’s equation gives a good estimation of \mathcal{L} , a better estimation could be $\mathcal{L} = \eta_C |_{\sigma_V = \sigma_{RPP}}$. The last expression relies on the same hypotheses as McFadden’s model, and still has the advantage of producing the value of \mathcal{L} even for non-stationary or non-calibrated data.

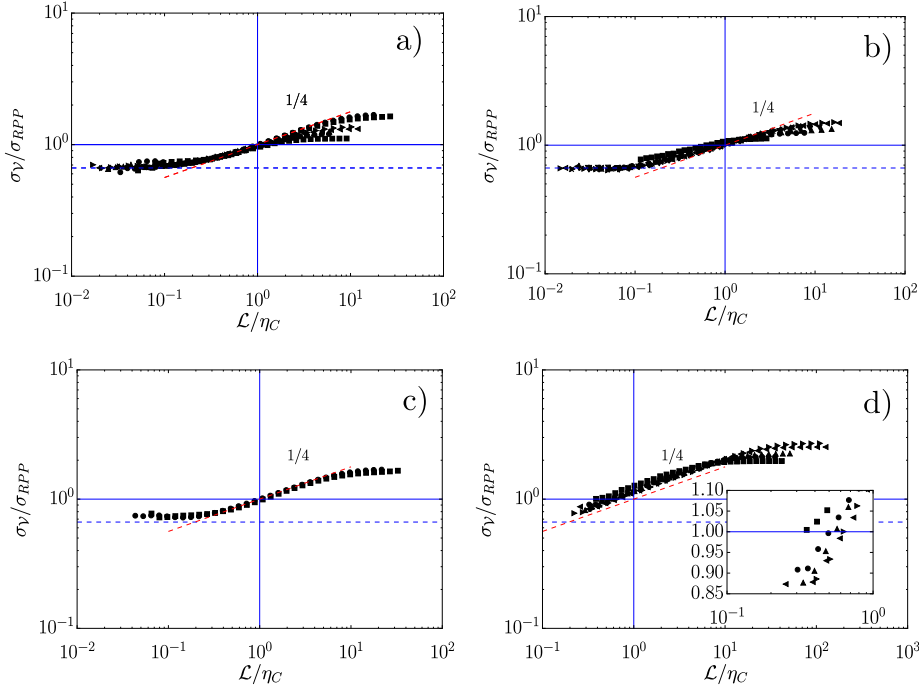


Fig. 4: Evolution of σ_V against the filter scale. Once more, in all cases \mathcal{L} has been obtained from the autocorrelation function. a) OG. b) PG. c) Wakes. d) AG. In d) we are only plotting the AG data for $\delta = 0.03$ (see figure 2d). In the figures the horizontal dashed line correspond to the standard deviation corresponding to a gaussian white noise process [13]; $\sigma_V / \sigma_{RPP} \approx 0.67$.

3.2.1 Zero crossing interval PDFs

The probability density function (PDF) of the inter-arrival distance between zero crossings from turbulent signals, and gaussian processes has been extensively studied in the last decades. Several studies retrieved that this PDF exhibits an exponential behaviour and clustering [23, 22]. Some studies have reported [4, 3] that the onset of such exponential cut-off present in the PDF is due to the randomisation effects (at scales larger than \mathcal{L}) that bend the coherent structures present in the flow reducing the probability of larger intervals between zero crossings.

Our analysis, by means of the 1D Voronoi tessellation, is consistent with those results: first, we retrieved an exponential cut off transition in our datasets PDFs (see figures 6a to 6d), as well as a power law behaviour (with an exponent close to ‘-5/3’) with increasing Re_λ . While it is not in the scope of this work, these figures suggest the possibility of using Voronoi tessellations to do a local analysis of the zero crossings cluster and voids properties (e.g. average cluster size) analogous to those conducted for inertial particles [14].

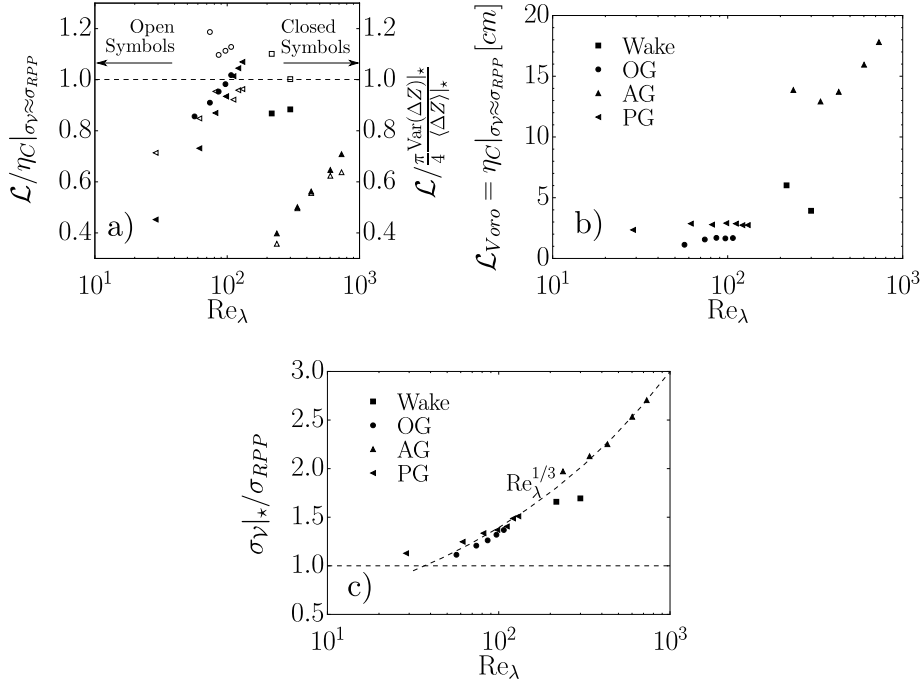


Fig. 5: Comparison between the two methods to estimate \mathcal{L} . a) Estimation of \mathcal{L} from $\mathcal{L}_{Voro} = \eta_C$ for which $\sigma_V \approx \sigma_{RPP}$, and from the value coming from equation 3 with respect to the integration of the autocorrelation up to its first ‘zero’. The \star represents the last value at the plateau of σ_V in figures 4a to 4d. b) Evolution of $\mathcal{L}_{Voro} = \eta_C |_{\sigma_V \approx \sigma_{RPP}}$ with Re_λ . c) Standard deviation of the Voronoi cells at the last point (filter) on the plateau. In the figures, we are only plotting the AG data for $\delta = 0.03$ (see also figure 2d).

4 Concluding remarks

The velocity autocorrelation function $\rho(r)$ coming from active-grid-generated flows may present a non-decaying behavior that could make ambiguous the estimation of \mathcal{L} by well-established methods. In the previous sections, our analysis of the variance of the distance between zero crossings of the fluctuating velocity via Voronoi tessellations in conjunction with the theoretical work of McFadden [13] allowed us to propose two methods to estimate the integral length scale \mathcal{L} . These methods are applicable to hot-wire records coming flows generated by active grids, and thereby, circumvent the problem of the non-standard behavior of $\rho(r)$. They are also consistent with values of \mathcal{L} estimated by traditional methods in several flows: turbulent wakes, and passive grids. The two methods have potential applications in field experiments where calibration could be difficult, or in particle laden flows, where under certain conditions, zero crossing analysis has been used to estimate the energy dissipation rate the presence of inertial particles [15]. Thus, our work

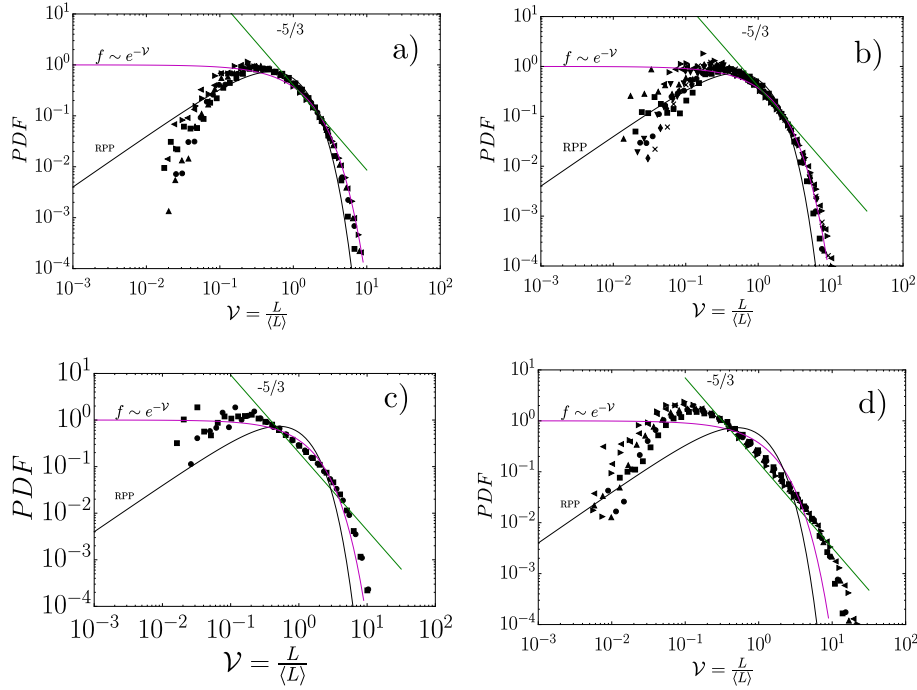


Fig. 6: PDF of the normalized Voronoï cell length $\mathcal{V} = L/\langle L \rangle$ for the last data point in the plateau (figures 4a to 4d) and the data found in table 1. a) OG. b) PG. c) Wakes. d) AG. In the figures the RPP label refers to a random Poisson process with no correlations at any scale [7, 14].

shows that all global turbulence parameters (such as ε , \mathcal{L} , λ ,...) can be estimated even with a non-calibrated hot-wire, provided that the mean velocity of the flow is known (needed for the Taylor hypothesis).

5 Acknowledgements

Our work has been partially supported by the LabEx Tec21 (Investissements d'Avenir - Grant Agreement # ANR-11-LABX-0030), and by the ANR project ANR-15-IDEX-02. The authors report no conflict of interest.

References

1. Bendat, J.S., Piersol, A.G.: Random data: analysis and measurement procedures, vol. 729. John Wiley & Sons (2011)
2. Bewley, G.P., Chang, K., Bodenschatz, E., for Turbulence Research), I.C.: On integral length scales in anisotropic turbulence. *Physics of Fluids* **24**(6), 061702 (2012)
3. Cava, D., Katul, G.G., Molini, A., Elefante, C.: The role of surface characteristics on intermittency and zero-crossing properties of atmospheric turbulence. *Journal of Geophysical Research: Atmospheres* **117**(D1) (2012)

4. Chamecki, M.: Persistence of velocity fluctuations in non-gaussian turbulence within and above plant canopies. *Physics of Fluids* **25**(11), 115110 (2013)
5. Dairay, T., Obligado, M., Vassilicos, J.C.: Non-equilibrium scaling laws in axisymmetric turbulent wakes. *Journal of Fluid Mechanics* **781**, 166–195 (2015)
6. Davila, J., Vassilicos, J.: Richardson’s pair diffusion and the stagnation point structure of turbulence. *Physical review letters* **91**(14), 144501 (2003)
7. Ferenc, J.S., Nédá, Z.: On the size distribution of poisson voronoi cells. *Physica A: Statistical Mechanics and its Applications* **385**(2), 518–526 (2007)
8. Gagne, Y., Castaing, B., Baudet, C., Malécot, Y.: Reynolds dependence of third-order velocity structure functions. *Physics of Fluids* **16**(2), 482–485 (2004)
9. Griffin, K.P., Wei, N.J., Bodenschatz, E., Bewley, G.P.: Control of long-range correlations in turbulence. *Experiments in Fluids* **60**(4), 55 (2019)
10. Hearst, R.J., Lavoie, P.: The effect of active grid initial conditions on high reynolds number turbulence. *Experiments in Fluids* **56**(10), 185 (2015)
11. Krogstad, P.Å., Davidson, P.: Freely decaying, homogeneous turbulence generated by multi-scale grids. *Journal of fluid mechanics* **680**, 417–434 (2011)
12. Mazellier, N., Vassilicos, J.: The turbulence dissipation constant is not universal because of its universal dependence on large-scale flow topology. *Physics of Fluids* **20**(1), 015101 (2008)
13. McFadden, J.: The axis-crossing intervals of random functions–ii. *IRE Transactions on Information Theory* **4**(1), 14–24 (1958)
14. Monchaux, R., Bourgoïn, M., Cartellier, A.: Preferential concentration of heavy particles: A Voronoi analysis. *Physics of Fluids* **22**(10) (2010). DOI 10.1063/1.3489987
15. Mora, D.O., Cartellier, A., Obligado, M.: Experimental estimation of turbulence modification by inertial particles at moderate re_λ . *Phys. Rev. Fluids* **4**, 074309 (2019). DOI 10.1103/PhysRevFluids.4.074309. URL <https://link.aps.org/doi/10.1103/PhysRevFluids.4.074309>
16. Mora, D.O., Muñiz Pladellórens, E., Riera Turró, P., Lagauzere, M., Obligado, M.: Energy cascades in active-grid-generated turbulent flows. *Phys. Rev. Fluids* **4**, 104601 (2019). DOI 10.1103/PhysRevFluids.4.104601. URL <https://link.aps.org/doi/10.1103/PhysRevFluids.4.104601>
17. Mydlarski, L.: A turbulent quarter century of active grids: from makita (1991) to the present. *Fluid Dynamics Research* **49**(6), 061401 (2017)
18. O’Neill, P.L., Nicolaides, D., Honnery, D., Soria, J., et al.: Autocorrelation functions and the determination of integral length with reference to experimental and numerical data. In: 15th Australasian fluid mechanics conference, vol. 1, pp. 1–4. Univ. of Sydney Sydney, NSW, Australia (2004)
19. Orey, S.: Gaussian sample functions and the hausdorff dimension of level crossings. *Zeitschrift für Wahrscheinlichkeitstheorie und verwandte Gebiete* **15**(3), 249–256 (1970)
20. Pope, S.B.: *Turbulent Flows*. Cambridge University Press (2000)
21. Puga, A.J., LaRue, J.C.: Normalized dissipation rate in a moderate taylor reynolds number flow. *Journal of Fluid Mechanics* **818**, 184–204 (2017)
22. Smith, J., Hopcraft, K., Jakeman, E.: Fluctuations in the zeros of differentiable gaussian processes. *Physical Review E* **77**(3), 031112 (2008)
23. Sreenivasan, K., Prabhu, A., Narasimha, R.: Zero-crossings in turbulent signals. *Journal of Fluid Mechanics* **137**, 251–272 (1983)
24. Sumbekova, S., Cartellier, A., Aliseda, A., Bourgoïn, M.: Preferential concentration of inertial sub-Kolmogorov particles: The roles of mass loading of particles, Stokes numbers, and Reynolds numbers. *Physical Review Fluids* **2**(2), 24302 (2017). DOI 10.1103/PhysRevFluids.2.024302
25. Tennekes, H., Lumley, J.L.: *A first course in turbulence*. MIT press (1972)
26. Tritton, D.J.: *Physical fluid dynamics*. Springer Science & Business Media (2012)
27. Valente, P., Vassilicos, J.C.: The decay of turbulence generated by a class of multiscale grids. *Journal of Fluid Mechanics* **687**, 300–340 (2011)
28. Vassilicos, J.C.: Dissipation in turbulent flows. *Annual Review of Fluid Mechanics* **47**, 95–114 (2015)